SEQUENTIALLY LINEAR SAW-TOOTH MODELLING OF REINFORCED STRUCTURES

J. G. Rots[1] and S. Invernizzi[2]
[1] Faculty of Architecture, Delft University of Technology, 2600 GA Delft, The Netherlands.
[2] Department of Structural and Geotechnical Engineering, Politecnico di Torino, 10129 Torino, Italy.

ABSTRACT

A sequentially linear saw-tooth continuum model which captures the nonlinear response via a series of linear steps is presented. In the model, the softening stress-strain curve with negative slope is replaced by a saw-tooth diagram of positive slopes, while the incremental-iterative procedure is replaced by a scaled sequentially linear procedure. Mesh-size objectivity is achieved by adjusting both the peaks and the ultimate strain of the saw-tooth diagram to the size of the finite elements, keeping the fracture energy invariant. First, considering large-scale dog-bone specimens in direct tension, it will be demonstrated that the model is capable of automatically providing the snap-back response. Furthermore, the bifurcation problem is circumvented as the scaling process triggers the lowest non-symmetric equilibrium path. Secondly, the model is extended from an isotropic to an orthotropic format, taking into account the direction of cracking and the anisotropy of the induced damage. In this way, the model can compare with classical fixed smeared crack models. This improvement allows for studying reinforced concrete structures, in which compressive struts develop parallel to the crack directions.

1 INTRODUCTION

Negative stiffness due to softening is a major problem in computational modeling of concrete fracture. It may lead to numerical instability and divergence of the incremental-iterative procedure. This holds especially for the analysis of medium- and large-scale structures. To try and solve such problems, users have to resort to arc-length or indirect control schemes, which are cumbersome and often inadequate when the peaks are irregular or the snap-backs sharp.

As an alternative, this paper presents a sequentially linear saw-tooth continuum model, which captures the nonlinear response via a series of linear steps. The softening stress-strain curve with negative slope is replaced by a saw-tooth diagram of positive slopes, while the incremental-iterative procedure is replaced by a scaled sequentially linear procedure [1] . After a linear analysis, the critical element, i.e. the element for which the stress is closest to the current peak in the saw-tooth diagram, is traced. Next, the stiffness of that element is reduced and the process is repeated. The sequence of critical states governs the global load-displacement response, while the elements with reduced stiffness reveal the softened areas. The advantage is that there is no such thing as ‘negative incremental stiffness’, as the secant linear (saw-tooth) stiffness is always positive. The analysis always ‘converges’. Mesh-size objectivity is achieved by adjusting both the peaks and the ultimate strain of the saw-tooth diagram to the size of the finite elements, keeping the fracture energy invariant [2] . In addition, the model is improved to take into account the intrinsic anisotropy due to crack nucleation and softening. This is a crucial aspect in order to describe reinforced structures, in which the reinforcement (*ties*) is balanced against compressive *struts* that develop parallel to the crack directions.

2 ISOTROPIC SAW-TOOTH SOFTENING

The basic idea is to look for the equilibrium configuration via secant approximations with restarts from the origin. The softening diagram is approximated by a saw-tooth curve and linear analyses

are carried out sequentially [1] . This is similar to procedures for fracture analysis on lattices [3] [4] , where little beam elements are removed rather than continuum elements reduced.

In a sequentially linear strategy, the softening diagram can be imitated by consecutively reducing Young's modulus E as well as the strength f_t ,. Young's modulus can e.g. be reduced according to:

$$E_i = \frac{E_{i-1}}{a}, \qquad \text{for } i = 1 \text{ to } N \tag{1}$$

with i denoting the current stage in the saw-tooth diagram, i-1 denoting the previous stage in the saw-tooth diagram and a being a constant. N denotes the amount of reductions that is applied in total for an element. When an element has been critical N times, it is removed completely in the next step. Please note that here we adopt the curve only as a 'mother' or envelope curve that determines the consecutive strength reduction in sequentially linear analysis. In the present study, attention is confined to a linear softening diagram, thus the ultimate strain ε_u of the diagram reads:

$$\varepsilon_u = \frac{2G_f}{f_t h}. \tag{2}$$

The reduced strength f_{ti} corresponding to the reduced Young's modulus E_i is taken in accordance with the envelope softening stress-strain curve. An advantage of the model is that the regular notions of fracture mechanics, like the principal tensile stress criterion, the envelope strength and fracture energy are maintained which helps in reaching realistic energy consumption and toughness as observed in experiments.

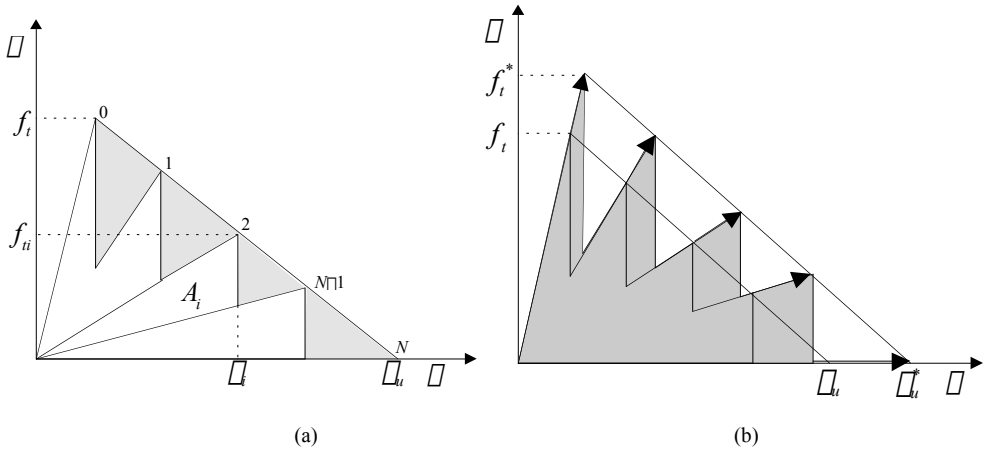

(a) (b)

Figure 1: Saw-tooth softening approximation scheme, the underestimated area is shown in gray (a). Regularization scheme with both the ultimate strain and the tensile strength update (b).

2.1 Mesh regularization

In order to achieve mesh-size objectivity, the ultimate strain ε_u in smeared crack models is usually adjusted to h according to Eq. (2) for linear softening [5] . In previous works [2] , it appeared that such adjustment is not sufficient to guarantee mesh-size objectivity for the case of the sequentially linear model. In fact, due to the saw-tooth approximation of the softening curve, the dissipated energy is always less than the theoretical one, i.e. the one referring to the smooth 'mother' softening curve (Fig.1a). The basic idea, thus, is to update the tensile strength, or the ultimate

strain, or even both, in order to keep the dissipated energy invariant. In other words, the area A^*, under the updated constitutive law, becomes invariant and equal to:

$$A^* = \frac{G_f}{h}. \tag{6}$$

Eq. 6 shows clearly that not only the number of teeth, but also the mesh size (i.e. the crack band width h) comes into play. Although in principle different approaches can be followed, it has been proved that the most effective technique is to update both the tensile strength and the ultimate strain. Therefore, the updated strength $f_t^*=kf_t$ and the ultimate strain $\varepsilon_u^*=k\varepsilon_u$ will be assigned, where the factor k can be determined [2] in such a way that the new area satisfies Eq. 6 (see Fig. 1b).

3 LARGE-SCALE DOG-BONE SPECIMENS IN DIRECT TENSION

The case study concern direct tensile tests carried out on large-scale dog-bone concrete specimens [6] . In order to prove the ability of the saw tooth model to capture the structural snap-back [7] [8], we considered the largest size among the entire series, denominated as *type F* (D=1600 mm; r=1160 mm). The mechanical parameters obtained by the test were adopted for the numerical analysis, i.e. a nominal tensile strength f_t=2.31 N/mm^2 and a fracture energy G_f=0.1411 N/mm. A linear softening tail was assumed.

3.1 Smeared crack nonlinear analysis

Boundary conditions were carefully taken into account modeling the central hinges at top and bottom used to de-constrain the structure. The influence of the boundary condition on post peak behavior is crucial [6] , both from an experimental and numerical point of view. The outcome of the numerical simulation depends on the control parameter. If the simulation is performed under load control, only the pre-peak branch of the load displacement curve can be traced. If the simulation is carried out with displacement control, on the other hand, the load displacement curve can be traced a bit further, till the snap-back phenomenon takes place. After that the analysis can be continued, but there is a sudden jump on the lower equilibrium path (i.e. snap-back). The third possibility is to adopt an indirect load control, e.g. with the arc-length methods [9] [10] . In this case, it is finally possible to obtain the whole load displacement curve.

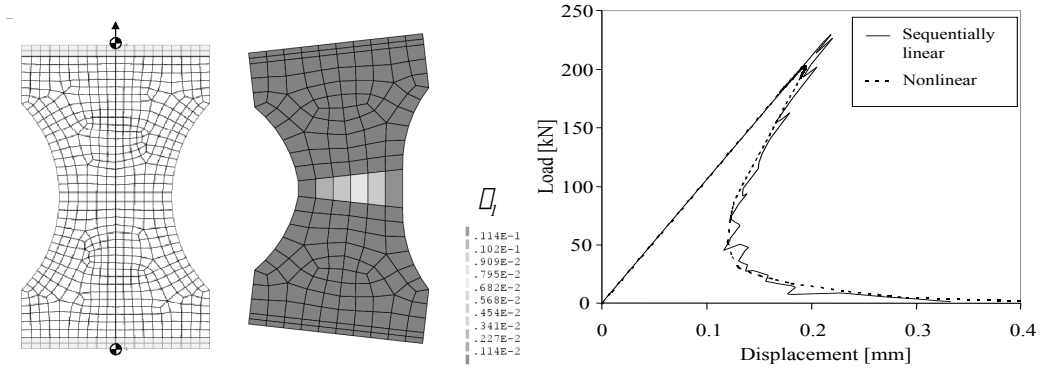

(a) (b) (c)

Figure 2: Mesh of the dog bone specimen (a); deformed mesh and principal tensile strain contour referring to the last sequentially linear step (b). Snap-back in the load displacement curve (c).

Unfortunately, the choice of load steps or of the arc-length options and indirect control parameters, is usually cumbersome, and difficulties increase with increasing the size (i.e. the brittleness) of the structure.

Another problem with the nonlinear analysis is the bifurcation. In fact, as soon as the peak load is reached, due to the symmetry of the structure, two different equilibrium paths arise. The symmetric path is unstable, and is not encountered experimentally, while the non-symmetric stable path is characterized by crack propagation from one side only of the dog-bone specimen. Consequently, a negative pivot arises, in the LDU scheme, due to the bifurcation of equilibrium, and it is necessary to introduce a perturbation of symmetry (geometrical or material) in the model, in order to get a solution.

3.2 Isotropic sequentially linear analysis

The same mesh and the same mechanical parameters were adopted for the saw tooth analysis (Fig. 3a). The analysis was carried out with a ten teeth approximation. The load displacement curve is depicted in Fig. 3c, and shows a very good agreement with the smeared crack nonlinear analysis. It is worth noting that both curves compare well with experimental results. The advantage of the sequentially linear analysis is that the system is always positive definite, so that a solution is always found at each step. The sequence of linear solutions automatically provides the snap-back.

When the solution is considered to be too coarse, showing an irregular spiky pattern, it is sufficient to refine the discretization, i.e. decreasing the mesh, or to increase the number of teeth.

Another advantage is that the numerical round-off implicitly breaks the symmetry of the model. There is no need to add imperfections to the model in order to follow the stable equilibrium path. At the same time, the indirect control of the structure is not required any more, since the effective control parameter is the propagating damage itself. The sequentially linear simulation provides not only the correct load displacement curve, but also the correct damage localization in the central part of the sample, induced by the dog-bone shape of the specimen (Fig. 3b).

4 ANISOTROPIC SEQUENTIALLY LINEAR: FIXED CRACKING

Although the isotropy assumption taken above allows for the simulation of cracking of plane concrete in direct tension or bending, a substantial improvement is necessary when dealing with reinforced concrete. In fact the isotropic reduction of stiffness does not represent the compressive struts that develop parallel to the cracks. Therefore, in analogy to the pioneering approach of [11] , the initial isotropic stress-strain law can be replaced by an orthotropic law upon crack formation, with the axes of orthotropy being determined according to a condition of crack initiation.

Referring to the plane stress situation, and to a local coordinate system oriented parallel to the crack plane, the following constitutive relation is assumed:

$$\begin{Bmatrix} \sigma_{nn} \\ \sigma_{tt} \\ \sigma_{nt} \end{Bmatrix} = \begin{bmatrix} \dfrac{E_i}{1-\beta^2\frac{E_i}{E}} & \dfrac{\beta E_i}{1-\beta^2\frac{E_i}{E}} & 0 \\ \dfrac{\beta E_i}{1-\beta^2\frac{E_i}{E}} & \dfrac{E}{1-\beta^2\frac{E_i}{E}} & 0 \\ 0 & 0 & \beta G \end{bmatrix} \begin{Bmatrix} \varepsilon_{nn} \\ \varepsilon_{tt} \\ \varepsilon_{nt} \end{Bmatrix}, \tag{8}$$

where n is the normal to the crack, t the crack plane, E_i the reduced Young modulus according to the sequentially linear scheme, and β the so-called shear retention factor.

Given the following transformations for the strain and stress vectors:

$$\begin{aligned} \boldsymbol{\sigma}_{nt} &= \mathbf{T}_{\sigma}(\alpha)\boldsymbol{\sigma}_{xy} \\ \boldsymbol{\varepsilon}_{nt} &= \mathbf{T}_{\varepsilon}(\alpha)\boldsymbol{\varepsilon}_{xy} \end{aligned}, \tag{9}$$

eq. 8 can be easily transposed in terms of global stress and strain components by pre- and post-multiplication with the transformation matrices:

$$\boldsymbol{\sigma}_{xy} = \mathbf{T}_{\sigma}^{-1}(\alpha)\mathbf{D}_{ns}\mathbf{T}_{\varepsilon}(\alpha)\boldsymbol{\varepsilon}_{xy}. \tag{10}$$

The above improved constitutive law was implemented in the general sequentially linear scheme.

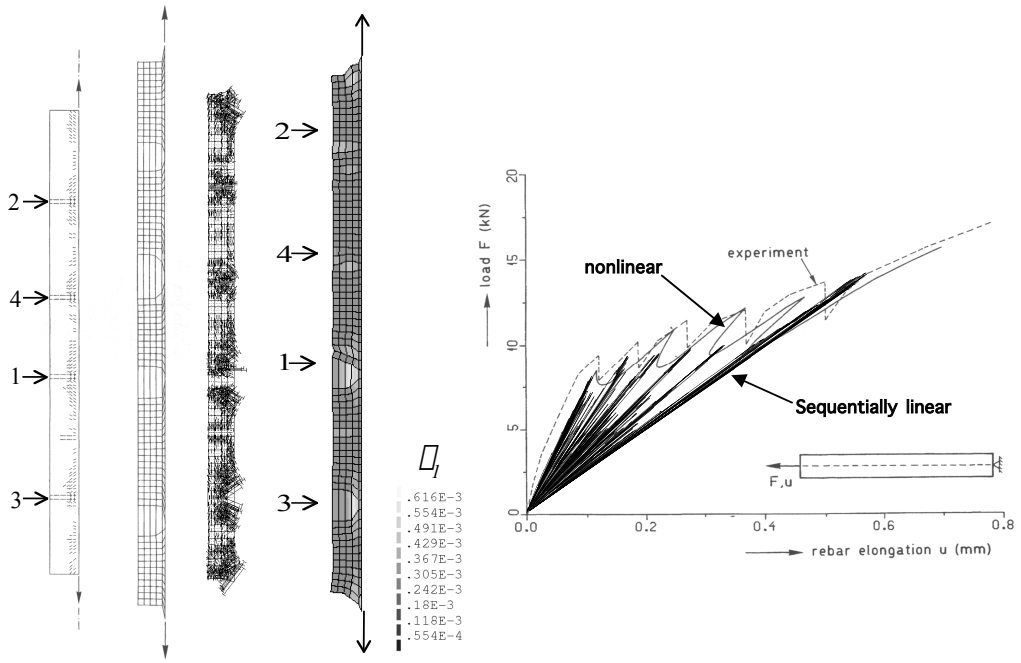

Figure 3: Long-embedment tension-pull specimen. Nonlinear cracking (a), nonlinear deformed mesh (b). Sequentially linear compressive struts (c) and deformation (d). Load-displacement curves: experimental [12] , nonlinear [13] and sequentially linear analysis (e).

4.1 Reinforced tension-pull specimen

A long-embedment tension-pull specimen is considered [12] . The steel is modeled by truss elements, and the concrete by axis-symmetry elements.

Perfect bond between steel and concrete was assumed. The strength of the concrete was assigned via a random generation of tensile strength (mean f_t=3.0 N/mm^2, standard deviation equal to 0.5 N/mm^2).

In Fig. 4e, results from nonlinear smeared analysis and experiments are compared with the load-displacement curve for the anisotropic sequentially linear model. Although the behavior is more brittle, the sequentially linear analysis is in good agreement with the nonlinear results, being able to describe snap-back and snap-through behavior. In Fig. 4a-d, the comparison is made in terms of crack localization and resulting deformed meshes. Four primary cracks emerge. In

particular, Fig. 4c shows how compressive struts arise in the anisotropic saw-tooth analysis. With the former isotropic version of the model, the struts (compressive cones) could not develop and an incorrect crack evolution was obtained.

5 CONCLUSIONS

The saw-tooth sequentially linear model has been reviewed in order to emphasize its ability to capture snap-back and snap-through instabilities automatically, without numerical problems. The model has thus been improved taking into account the damage anisotropy induced by cracking. The effectiveness of the model to capture basic features of reinforced structures has been evaluated by the example of the long-embedment tension-pull test.

6 ACKNOWLEDGEMENTS

Financial support from Delft Cluster, COB, Netherlands Technology Foundation STW, as well as the Italian Ministry of University and Scientific Research MIUR and of the European Union EU is acknowledged. The research was carried out using an adapted version of DIANA.

7 REFERENCES

[1] Rots, J.G. 2001. Sequentially linear continuum model for concrete fracture. In de Borst R., Mazars J., Pijaudier-Cabot G., van Mier J.G.M. (eds), *Fracture Mechanics of Concrete Structures*: 831-839. Lisse: Balkema

[2] Rots, J.G. & Invernizzi S. 2003. Regularized saw-tooth softening, In Bicanic N., de Borst R., Mang H., Meschke G. (eds), *Computational Modelling of Concrete Structures*: 599-617. Lisse: Balkema.

[3] Schlangen, E. & van Mier J.G.M. 1992. Experimental and numerical analysis of micro-mechanisms of fracture of cement-based composites. *Cement & Concrete Composites* 14: 105-118.

[4] Beranek, W.J. & Hobbelman, G.J. 1995. 2D and 3D-Modelling of concrete as an assemblage of spheres: revaluation of the failure criterion. In Wittmann F.H. (ed.), *Fracture mechanics of concrete structures. Proc. FRAMCOS-2*: 965-978. Freiburg: Aedificatio.

[5] Bazant, Z.P. & Oh, B.H. 1983. Crack band theory for fracture of concrete. *Materials and Structures* 16(93): 155-177.

[6] Van Vliet, M.R.A. 2000. *Size effect in tensile fracture of concrete and rock.* PhD Thesis, Delft University of Technology.

[7] Carpinteri A. 1984. Interpretation of the Griffith instability as a bifurcation of the global equilibrium, *NATO Advanced Workshop on Application of Fracture Mechanics to Cementitious Composites*, P. Shah (ed.), Martinus Nijhoff, 287-316.

[8] Carpinteri A., Monetto I. 1999. Snap-Back analysis of fracture evolution in multi-cracked solids using boundary element method, *International Journal of Fracture*, 98: 225-241.

[9] Crisfield, M.A. 1984. Difficulties with current numerical models for reinforced-concrete and some tentative solutions. F. Damjanic, N. Bicanic et al. (eds), *Proc. Int. Conf. Computer Aided Analysis and Design of Concrete Structures*. Part I: 331-358.

[10] de Borst, R. 1987. Computation of post-bifurcation and post-failure behavior of strain-softening solids. *Computers & Structures* 25(2): 211-224.

[11] Rashid, Y.R. 1968. Analysis of prestressed concrete pressure vessels, *Nuclear Engng. And Design* 7(4): 334-344.

[12] Gijsbers, F.B.J. & Hehemann, A.A. 1977. Some tensile tests on reinforced concrete, *Report BI-77-61*, TNO Inst. For Building Mat. And Struct., Delft.

[13] Rots, J.G. 1985. Bond-slip simulations using smeared cracks and/or interface elements. *Res. Report 85-01, Struct. Mech.*, Dept. of Civil Engng., Delft Univ. of Techn.